# Photoinduced Energy and Electron Transfer in a Giant Zinc Porphyrin−Bridge−$C_{60}$ System†

**Toby D. M. Bell,‡ Kenneth P. Ghiggino,*,‡ Katrina A. Jolliffe,§ Millagahamada G. Ranasinghe,§ Steven J. Langford,§ Michael J. Shephard,§ and Michael N. Paddon-Row*,§**

*School of Chemistry, University of Melbourne, Victoria, Australia, 3010, and School of Chemistry, University of New South Wales, Sydney, Australia, 2052*

*Received: November 13, 2001; In Final Form: July 23, 2002*

Photoinduced electronic energy transfer (EET) and electron transfer (PET) have been investigated in a multichromophoric system **2**, that comprises zinc porphyrin (ZnP), dimethoxynaphthalene, and [60]fullerene ($C_{60}$) chromophores separated by norbornylogous bridge sections of six and five bond lengths, respectively. In toluene as solvent, EET from ZnP to $C_{60}$ occurs in folded and extended conformations of the molecule with rate constants of $1.3 \times 10^{10}$ and $8.1 \times 10^{8}$ $s^{-1}$, respectively. Evidence is presented for the existence of a third collapsed conformation of **2** which can undergo PET with a rate constant of $1.1 \times 10^{12}$ $s^{-1}$. In benzonitrile solvent, PET can also occur in the folded and extended geometries leading to a charge separated lifetime of 460 ns. The mechanisms for the unusually complex solvent and conformationally dependent excited-state processes in this molecule are discussed.

## Introduction

Organic molecules containing electron donating and accepting chromophores have been studied extensively over the past few decades to model and mimic the photoinduced electron-transfer processes of natural photosynthesis.[1−6] Recently, [60]fullerene ($C_{60}$) has been incorporated in a number of such systems, and the use of $C_{60}$ as a component in future molecular photovoltaic devices is an area of intense current research activity.[7−22] The $C_{60}$ chromophore has many desirable properties: it can accept a number of electrons (up to six)[23] with an associated low reorganization energy,[24,25] it can act as an energy trap,[26] it is highly symmetrical, and it can be readily functionalized and incorporated into larger molecular structures.[27−38] As a component of donor−bridge−acceptor molecules, $C_{60}$ has been successfully used in achieving one of the key requirements for artificial photosynthesis, namely, that of generating long-lived charge separated (CS) states.[26,39−51]

We have reported previously[26] on the photophysics of the ZnP−$C_{60}$ dyad **1**, in which the two chromophores are separated by a nine bond norbornylogous bridge.[52] In this previous study, rapid photoinduced electron transfer (PET) was observed upon excitation in benzonitrile ($k_{cs} = 1 \times 10^{10}$ $s^{-1}$). The resultant CS state, $^{\bullet+}$ZnP−$C_{60}^{\bullet-}$ exhibited a lifetime of 420 ± 20 ns. In the nonpolar solvent toluene, the CS state is of too high an energy to be generated from photoexcited ZnP. However, steady-state fluorescence emission from **1** was still quenched substantially with respect to a ZnP model compound. The observation of sensitized $C_{60}$ fluorescence emission indicated that electronic energy transfer (EET) was operative in this solvent.[26]

In light of the interesting results for **1**, multichromophoric systems comprising the same respective terminal chromophores with the addition of a dimethoxynaphthalene (DMN) chromophore as part of the linking bridge were synthesized.[53] The spectroscopic and redox properties of DMN preclude it from participating as either an energy or electron relay intermediary from electronically excited porphyrin. However, DMN can facilitate electronic coupling between the donor and acceptor terminals through superexchange[54] and modify the relative structural arrangement of the porphyrin and $C_{60}$ chromophores. Our strategy in this work is to characterize and compare the photophysical behavior of **1** and **2** in polar and nonpolar solvents to elucidate the role of such structural modification. The structures of these two molecules and of model monochromophoric compounds **3** and **4** are shown in Figure 1.

AM1 gas-phase calculations[26,53] suggest that there are two conformations available to **1** and **2** due to flipping of the cyclohexene ring which forms the first bridge unit immediately adjacent to the $C_{60}$ chromophore. These conformations are referred to as "folded" and "extended" and are shown in Figure 2 for both **1** and **2**. The center-to-center distances between the ZnP and $C_{60}$ chromophores in the folded and extended arrangements of the two molecules are 15.3 and 20.4 Å for **1** and 13.5 and 19.4 Å for **2**. The shortest distances between the surface of the $C_{60}$ unit and the base of the porphyrin ring in the folded and extended conformations of these molecules are 9.0 and 13.6 Å, for **1**, and 8.0 and 14.3 Å, for **2**. The two conformers of each molecule are almost degenerate with the extended arrangement being favored in both compounds, by 0.2 kcal/mol for **1** and 0.14 kcal/mol for **2**.

Calculation of the kinetic barrier between the folded and extended arrangements has not been attempted for these molecules. However, barriers calculated for such a ring-flipping process in a series of similar $C_{60}$ containing dyads are of the order of 8−10 kcal/mol.[28,55] It was also found that the calculated barrier was largely independent of the bridge length or the nature of the other chromophore. For example, the energy barrier separating the two arrangements calculated for a $C_{60}$−naphthoquinone(NQ) dyad with an 11 bond bridge is 9.8 kcal/

† Originally submitted for the "G. Wilse Robinson Festschrift", *J. Phys. Chem. A* **2002**, *106* (No. 33).

* To whom correspondence should be addressed.
‡ University of Melbourne.
§ University of New South Wales.

10.1021/jp014155k CCC: $22.00 
Published on Web 10/08/2002

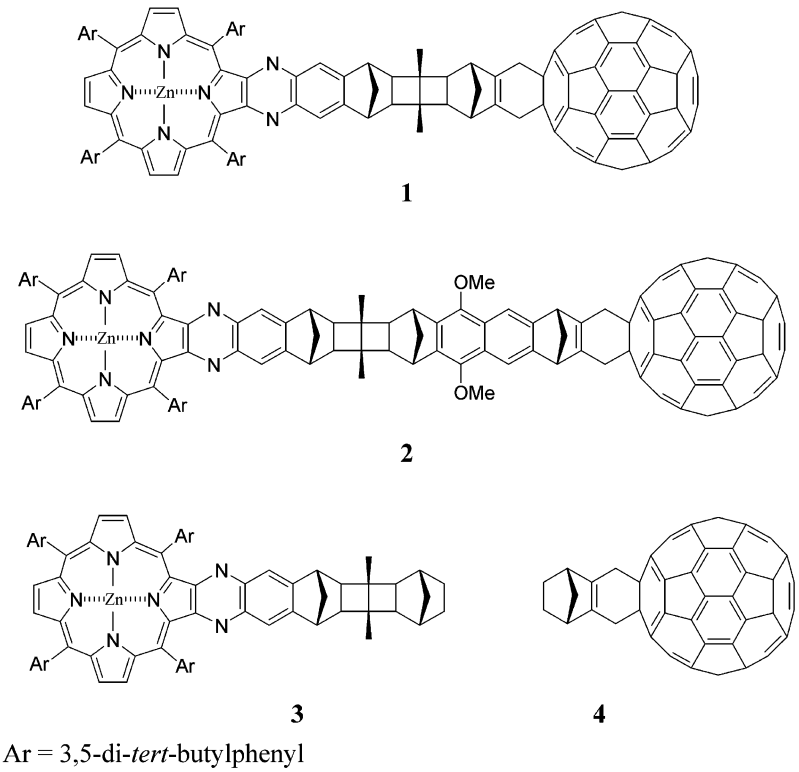


**Figure 1.** Structures of ZnP−$C_{60}$ (**1**), ZnP−DMN−$C_{60}$ (**2**), and the ZnP and $C_{60}$ model compounds, (**3** and **4**).

mol.[55] Barriers of comparable magnitude are expected for **1** and **2**, and they would therefore make interconversion between the two conformers of each slow with respect to the time frame of singlet excited-state processes of the ZnP chromophore. It is demonstrated in this work that such conformational complexity is a major factor in determining the efficiency and dynamics of energy and electron-transfer processes in these molecules.

## Experimental Section

Synthesis of all compounds has been reported previously.[53,56] Solvents were spectroscopic grade, and solutions were degassed by multiple freeze−pump−thaw cycles before measurements. Absorption spectra were recorded on a Varian Cary 50 absorption spectrophotometer, and steady-state fluorescence emission spectra were recorded on a Varian Eclipse spectrofluorimeter. Fluorescence decay profiles were obtained by the time correlated single photon counting technique (TCSPC) using a mode-locked and cavity-dumped dye laser (Spectra-Physics 3500) as the excitation source. The total instrument response function is ca. 80 ps fwhm, and fluorescence decay profiles were analyzed using reconvolution routines based on the Marquardt algorithm.[57] Fitted functions were assessed by the magnitude of the reduced chi-square ($\chi^2$) and Durban−Watson (DW) fitting parameters and by inspection of weighted residuals. Transient absorption measurements utilized a flash photolysis apparatus incorporating a Nd:YAG laser pumping an optical parametric oscillator (Continuum NY61/Cassix OPO BBO-3B) providing 7 ns pulses at 570 nm for excitation of the samples and a xenon lamp analyzing source. Excitation energies were kept below 5 mJ to minimize second-order effects. Transient spectra (and time-gated fluorescence emission spectra) were obtained using a spectrograph (Acton Research Corporation SpectraPro-300i) and intensified CCD camera (Princeton Instruments ICCD-MAX). Transient decays were recorded using a photomultiplier tube/digital oscilloscope (Hamamatsu R928/Tektronix TDS-520) and analyzed as outlined elsewhere.[26,58] The HF/3-21G geometry optimization of the folded conformation of **2** was carried out using Gaussian 98.[59]

## Results

The absorption spectrum of the ZnP chromophore is characterized by a strong Soret band absorption ($\epsilon \sim 10^4$ mol$^{-1}$ m$^{-2}$) in the wavelength region 400−480 nm and a series of weaker ($\epsilon \sim 10^3$ mol$^{-1}$ m$^{-2}$) Q-band absorptions located in the range 520−640 nm. $C_{60}$ absorption is predominantly in the UV region, although absorption does tail through the whole visible spectrum, but it is very weak ($\epsilon < 10^2$ mol$^{-1}$ m$^{-2}$). The spectrum of **1** is well represented as the sum of the component model compounds **3** and **4**. The spectrum of **2** is somewhat different. Both the Soret and Q-bands show significant broadening, and the absorption maxima are red-shifted by 3 nm. Absorption spectra of all compounds in toluene are shown in Figure 3.

Steady-state fluorescence spectra of **1**, **2**, and **3** in toluene (see Figure 4) show a large degree of quenching for both **1** and **2** with respect to the model porphyrin **3** (75% and 92%, respectively). Time-gated fluorescence emission spectra are shown in Figure 5 parts a and b. These spectra are recorded at a time delay such that the majority of the ZnP fluorescence has decayed away thus highlighting the longer-lived emitting components. The spectra reveal the presence of additional emissions in the near infrared (NIR) region of the spectrum for compounds **1** and **2** compared to the ZnP model **3**. In Figure 5a, which shows the fluorescence spectra for the dyad **1** and the ZnP model **3** overlaid, additional bands with maxima at approximately 715 and 800 nm for **1** are clearly evident. The fluorescence emission spectrum of the $C_{60}$ model **4** is included for reference, and it features a main peak near 715 nm and a smaller peak near 800 nm, which is consistent with spectra reported for the parent $C_{60}$ molecule.[23] Thus, the fluorescence bands at 715 and 800 nm from **1** are assigned to $C_{60}$ emission. Very similar characteristic $C_{60}$ emission was seen by Imahori et al.[60] for another ZnP−$C_{60}$ dyad in toluene. Figure 5b shows

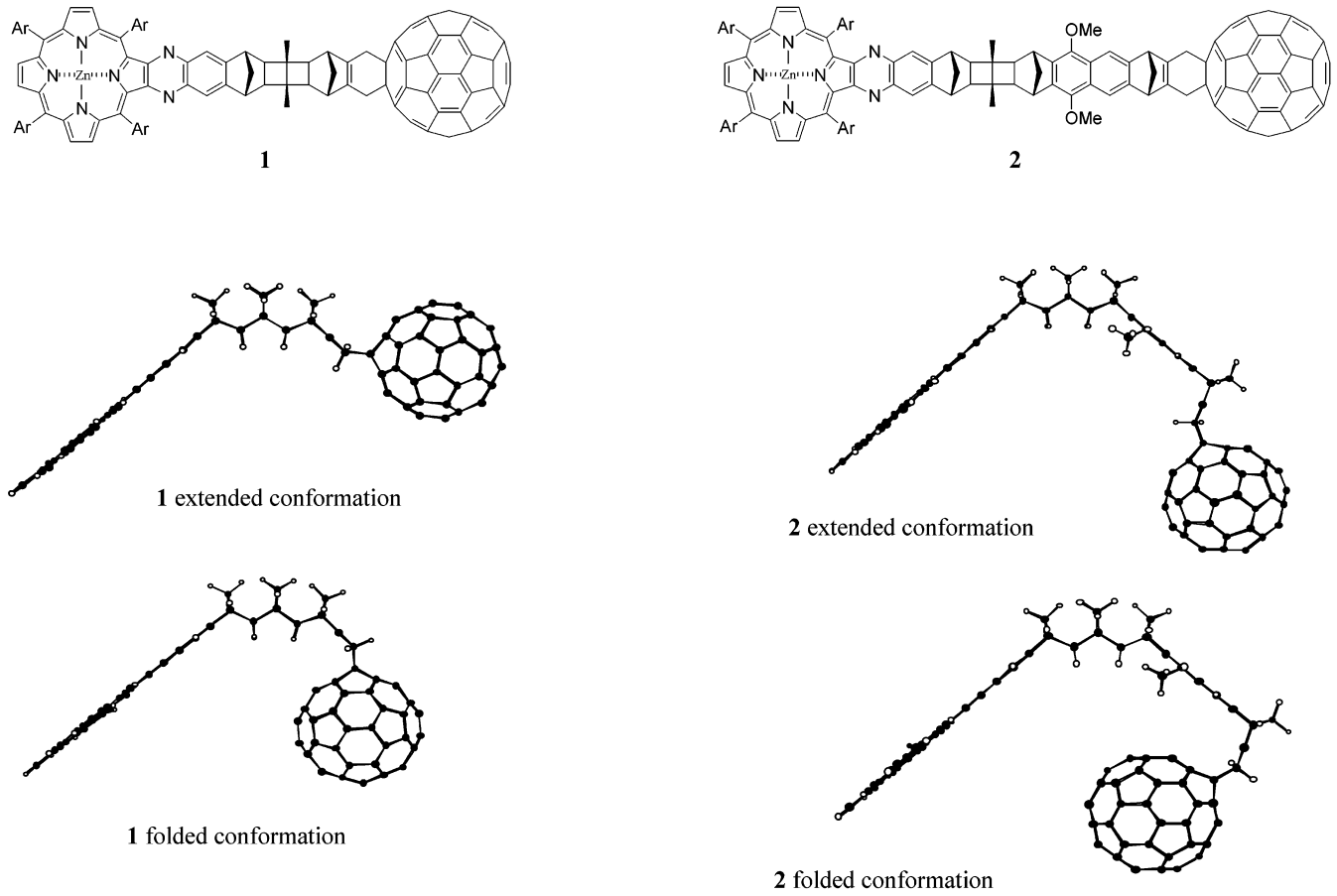


**Figure 2.** Profiles of the AM1 optimized structures of the extended and folded conformations of **1** (left) and **2** (right) in which Ar = H. The extended and folded conformations arise from "flipping" of the cyclohexene ring adjacent to the $C_{60}$ chromophore in each molecule. The extended conformer is favored by 0.20 kcal/mol for **1** and by 0.14 kcal/mol for **2**. The center-to-center distances are 20.4 and 15.3 Å for the conformers of **1** and 19.4 and 13.5 Å for the conformers of **2**.

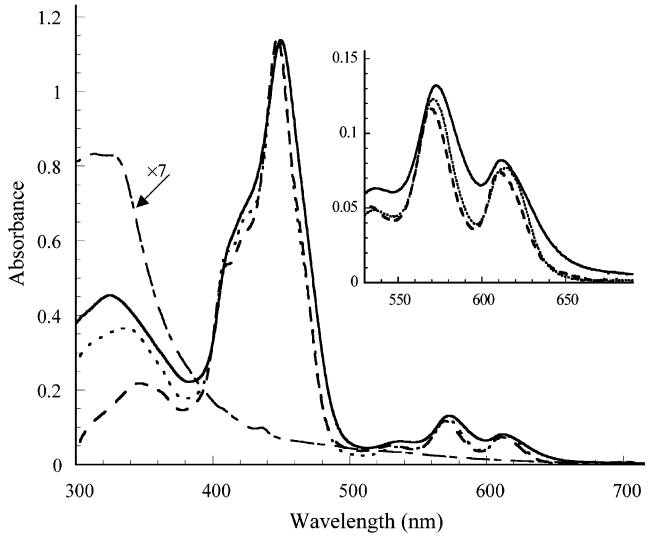


**Figure 3.** Absorption spectra of **1** (···), **2** (−), and **3** (- - -) and the $C_{60}$ model **4** (·−·) in toluene. The inset shows the Q-band region of **1**, **2**, and **3** enlarged. The spectrum of **4** was recorded for a solution approximately seven times as concentrated as those of **1**, **2**, and **3**.

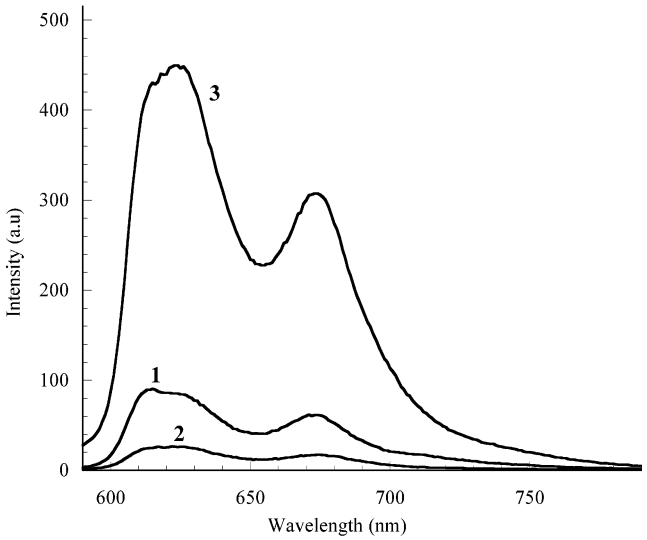


**Figure 4.** Steady-state fluorescence emission of **1**, **2**, and **3**, in toluene. Excitation was at 570 nm, and the spectra are uncorrected.

a late gated fluorescence emission spectrum of **2** in toluene with the spectra of **1** and **3** included for comparison. A band due to emission from the $C_{60}$ moiety is present as noted for **1**; however, there is a further broad emission band centered at 840 nm. A similar fluorescence band has been observed in some other ZnP and $C_{60}$ containing systems and assigned to charge transfer (CT) fluorescence arising from a close contact pair of ZnP and $C_{60}$ in the ground state.[61,62]

Time-resolved fluorescence decay profiles of the model compounds **3** and **4** recorded by the TCSPC technique were fitted by single-exponential functions with decay lifetimes of 1.20 and 1.46 ns, respectively. The extracted lifetime of 1.46 ns for **4** agrees with values reported for similar functionalized $C_{60}$ model compounds in toluene.[27,48,60] Compounds **1** and **2**

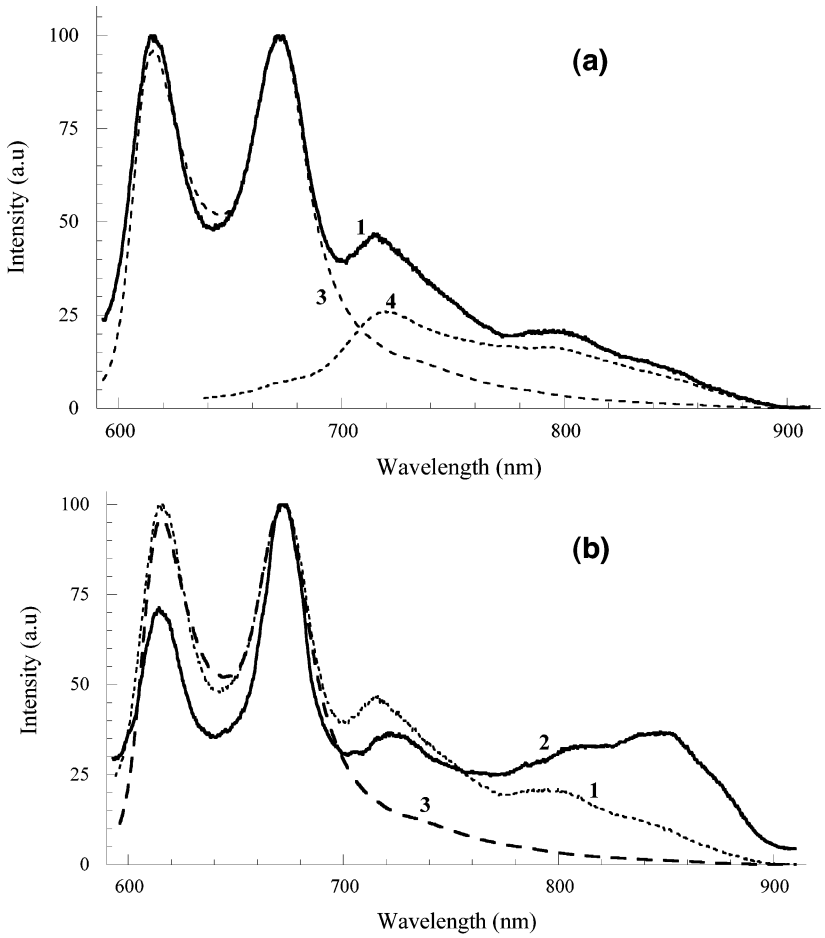


**Figure 5.** a. Time-gated (12 ns gate delay, 2ns gate width) fluorescence emission spectra in toluene of the model compounds **3** and **4** and the dyad **1**. Emission from **1** and **3** are normalized at 675 nm. Emission from **4** has been magnified many times. Excitation of **4** was at 490 nm and **1** and **3** at 570 nm. Sensitized $C_{60}$ emission is clearly evident in the spectrum of **1**. b. Time-gated (10 ns gate delay, 2ns gate width) fluorescence emission spectrum of **2** in toluene following excitation at 570 nm. The spectra of **1** and **3** from Figure 5a are included for comparison. For **2**, sensitized $C_{60}$ fluorescence and an additional band, attributed to charge-transfer fluorescence and centered at 840 nm, are also present.

**TABLE 1: Fitted Lifetimes ($\tau$), Percentage Contributions of Each Lifetime (%$\tau$), and Goodness-of-Fit Parameters ($\chi^2$ and DW) for Time Correlated Single Photon Counting (TCSPC) Fluorescence Decay Profile Analysis of Compounds 1−4 in Toluene**

| | $\tau_1$ (ns) | $\tau_2$ (ns) | $\tau_3$ (ns) | % $\tau_1$ | % $\tau_2$ | % $\tau_3$ | $\chi^2$ | DW |
|---|---|---|---|---|---|---|---|---|
| $P_{Zn}$ model (**3**)[a] | 1.20 | | | 100 | | | 1.18 | 1.92 |
| $C_{60}$ model (**4**)[b] | 1.46 | | | 100 | | | 1.25 | 1.79 |
| ZnP−$C_{60}$ (**1**)[a] | 0.156 | 0.486 | 1.42 | 63 | 32 | 5 | 0.93 | 1.81 |
| ZnP−DMN−$C_{60}$ (**2**)[a] | 0.070 | 0.607 | 1.63 | 41 | 48 | 11 | 0.93 | 2.02 |

[a] Fluorescence emission monitored at 675 nm. [b] Fluorescence emission monitored at 720 nm.

required triple exponential functions for adequate fits. The fitted lifetimes, percentage contributions of each component, and "goodness-of-fit" parameters, $\chi^2$ and DW, are presented in Table 1. The rate constants for the competing nonradiative processes derived from the two shortened fitted lifetimes are $1.3 \times 10^{10}$ and $8.1 \times 10^8$ $s^{-1}$ for **2** and $5.6 \times 10^9$ and $1.2 \times 10^9$ $s^{-1}$ for **1**. The third, longer lifetime component contributes only a small proportion of the total fluorescence counts and has a lifetime similar to the model compounds **3** and **4**. It is attributed to weak $C_{60}$ fluorescence and possibly to a trace amount of molecules containing a ZnP chromophore but lacking the $C_{60}$ acceptor.

Transient absorption spectra of the model compounds **3** and **4** (not shown) show absorptions that result from the formation of triplet states via intersystem crossing (ISC) after excitation. The triplet state of the ZnP containing model system **3** absorbs with a maximum at 500 nm and weakly throughout the longer wavelength region of the visible spectrum. The triplet state of the cyclohexyl-fused $C_{60}$ moiety, **4**, has a characteristic absorption band centered at 700 nm.[27,39,48] These triplet absorptions (denoted $^3$ZnP and $^3C_{60}$, respectively) have relatively long lifetimes: 270 $\mu$s for $^3$ZnP and 20 $\mu$s for $^3C_{60}$. The transient absorption spectra of **1** and **2** in toluene show the same spectral features with two absorption bands centered at 500 and 700 nm. By comparison with the transient spectra of the model compounds **3** and **4**, the 500 nm band can be assigned to $^3$ZnP and the 700 nm band to $^3C_{60}$. However, the temporal behavior of the transient species is very different for the two compounds. The surfaces shown in Figure 6 parts a and b each comprise 30 transient absorption spectra of **1** and **2** in toluene, respectively, with each spectrum successively delayed by 2 $\mu$s from the excitation pulse. Visual inspection of parts a and b of Figure 6 shows that the transient species of **2** decay much more rapidly than for **1**. Also noteworthy is the difference in the magnitudes of the transient absorbance of **1** and **2**. The spectra were recorded under similar conditions (same solution absorbance and excitation pulse power) yet the transient absorbance for **2** is only about half that of **1**.

In the polar solvent benzonitrile, the absorption spectrum of **2** is again broadened through the Q-band region of the spectrum and red-shifted with respect to the absorption spectra of **1** and **3**. Steady-state fluorescence emission from **2** is quenched by

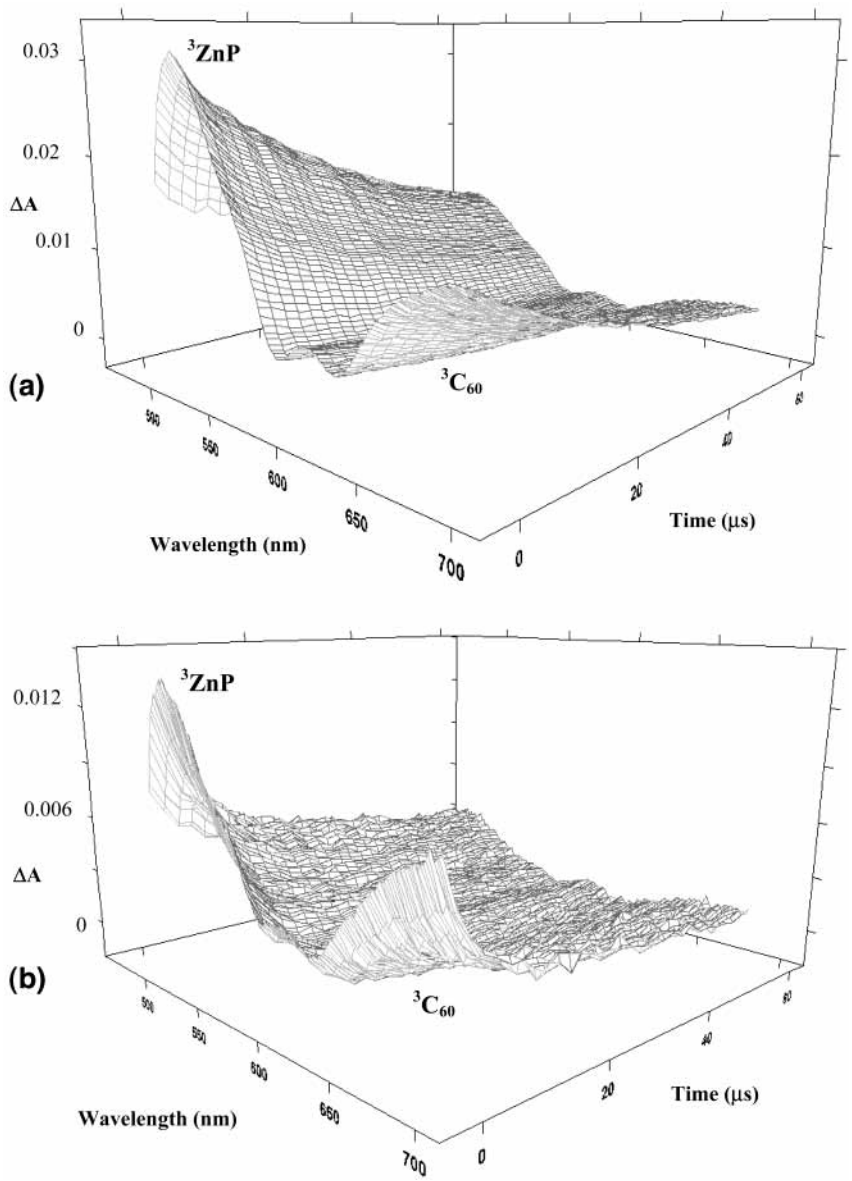


**Figure 6.** Three-dimensional plots of 30 transient absorption spectra of **1** (Figure 6a) and **2** (Figure 6b) in toluene. The time interval between each spectrum is 2 $\mu$s. Excitation was at 570 nm, and the gate width for each spectrum was 1 $\mu$s.

97% with respect to **3**. Time-gated fluorescence emission spectra did not reveal any sensitized $C_{60}$ emission or any CT emission from **2** for wavelengths out to 900 nm. The dyad **1** also does not show any sensitized $C_{60}$ emission in benzonitrile where PET is known to be an efficient deactivation process.[26] The TCSPC fluorescence decay profile of **2** in benzonitrile could be fitted by a triple exponential decay function with lifetimes of 0.149, 0.582, and 1.56 ns with each component contributing 49%, 35%, and 16% of the initial intensity, respectively. Using the previously determined[63] lifetime of 1.35 ns for **3** in benzonitrile, the two shorter components correspond to competing nonradiative quenching processes for two species with rate constants of $6.0 \times 10^9$ and $9.8 \times 10^8$ $s^{-1}$.

It has been previously shown for **1** in benzonitrile that efficient through bond (TB) PET from ZnP to $C_{60}$ is the dominant fluorescence quenching process leading to the observation of $ZnP^{\bullet+}$ in the transient absorption spectrum.[26] The transient absorption spectrum for **2** recorded in benzonitrile is shown in Figure 7a and for **1** in Figure 7b for comparison.[64] The broad absorption in the 600−700 nm region is characteristic of $ZnP^{\bullet+}$ in agreement with previous assignments.[26,48,60] Such an absorption band is not observed for the ZnP model **3**. A significant observation is the reduced yield of the $ZnP^{\bullet+}$ transient in **2** compared to **1**. The transient decay profile of **2** recorded at 670 nm could be best fitted by three decay components with lifetimes (and initial contributions to the transient absorbance) of 460 ns (58%), 6 $\mu$s (15%), and 87 $\mu$s (27%).

## Discussion

In toluene, the observations of sensitized $C_{60}$ fluorescence emission and the formation of $^3C_{60}$ upon excitation of **1** and **2** at 570 nm where the ZnP chromophore absorption strongly dominates demonstrates that efficient transfer of the excitation energy from the ZnP chromophore to $C_{60}$ is taking place. For an equimolar solution of the two model compounds **3** and **4**, excitation at 570 nm leads to no detectable emission from $C_{60}$. This is expected as the extinction coefficient for the ZnP chromophore at this wavelength is 16 times higher than that for $C_{60}$, and the fluorescence quantum yield of $C_{60}$ is approximately 2 orders of magnitude lower than for ZnP.[23] However, for the bridged compounds **1** and **2**, a band arising from $C_{60}$ fluorescence, though weak, is readily observable (cf.

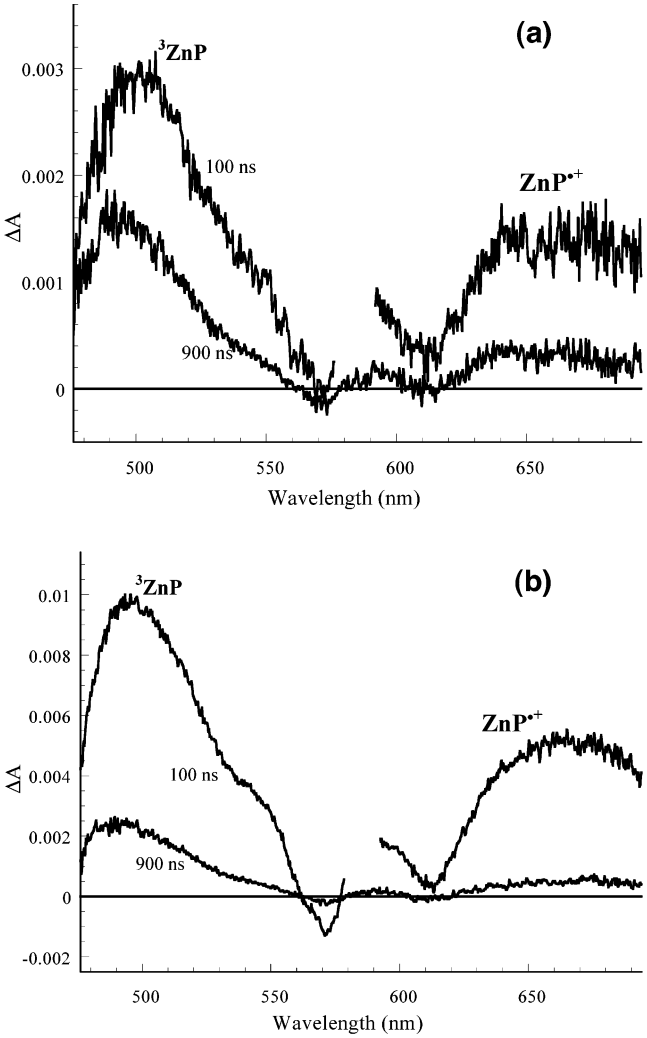


**Figure 7.** Transient absorption spectra of **2** (Figure 7a) and **1** (Figure 7b) in benzonitrile recorded at 100 and 900 ns after excitation at 575 nm with a gate width of 100 ns. The solutions of **2** and **1** were of similar optical densities yet the magnitude of the transient absorption of **2** is much less than that of **1**. The break in the early gated spectra is due to omission of scattered laser light.

parts a and b of Figure 5). Further evidence that efficient EET occurs from ZnP to $C_{60}$ in **1** and **2** is provided by fluorescence excitation spectra. Excitation spectra for $C_{60}$ fluorescence monitored at 720 nm show a close correspondence with the ZnP absorption spectrum indicating that light absorbed by the porphyrin is emitted from the $C_{60}$ chromophore.

The existence of two conformers for **1** and **2**, the folded and extended geometries predicted by the AM1 calculations illustrated in Figure 2, can explain the result that two shortened fluorescence lifetime components are required to obtain a satisfactory fit of the fluorescence decays in toluene. These conformers must interconvert on a time-scale that is slow compared to the fluorescence process. Because the donor−acceptor (ZnP−$C_{60}$) separations are different for the two conformations of **1** and **2**, the conformers can be expected to exhibit different rate constants for through-space dipole−dipole EET. The EET rate constants derived from the lifetime data are $1.3 \times 10^{10}$ and $8.1 \times 10^{8}$ $s^{-1}$ for **2** and $5.6 \times 10^{9}$ and $1.2 \times 10^{9}$ $s^{-1}$ for **1**. For each molecule, the smaller of the two rate constants is assigned to EET in the extended conformation and the larger rate constant to EET in the folded conformation.

In addition to EET being a quenching mechanism for **2** in toluene, the experimental evidence indicates that an ultrafast PET process is operative in **2** but not in **1**. The fluorescence emission band in the NIR centered at 840 nm for **2** is characteristic of CT fluorescence and indicates the presence of a fast CS process. In addition, the degree of quenching implied by the fluorescence emission decay data and steady-state fluorescence measurements are consistent for **1** but not for **2**. The degree of quenching can be determined by comparison of the integrated areas under steady-state spectra (for solutions of the same absorbance) and by comparison of the integrals of the fitting functions derived from time-resolved fluorescence emission decay profiles. For **1** with respect to the model porphyrin **3**, the extent of quenching implied by the two estimates is approximately the same. However, for **2** compared to **3**, the steady-state emission is reduced by 92%, but the integral of the fitting function extracted for **2** from its fluorescence decay profile is 40% that of **3**. This indicates the presence of a quenching mechanism that is operating on a time scale too rapid to be detected by the TCSPC time-resolved apparatus (<20 ps). The observation that the magnitude of the transient absorptions of **2** are considerably lower than those observed for **1** for solutions having the same absorbance provides further evidence that there is an additional ultrafast process taking place which quenches a significant proportion of the excited ZnP chromophores of **2**.

Recent femtosecond fluorescence upconversion experiments[65] on **2** in toluene recorded over a 50 picosecond time range have revealed an ultrafast component with a lifetime of 880 fs ($k_{cs} = 1.1 \times 10^{12}$ $s^{-1}$) which contributes 42% of the initial intensity. The very short-lived component of the fluorescence emission of **2**, in addition to the two components recorded using the lower time-resolution TCSPC technique (assigned to the folded and extended conformations of **2**), is evidence for the existence of a third, slowly interconverting conformation of **2**. This conformation must have a much more compact structure than the folded and extended conformations in order to account for the subpicosecond PET process. Such a geometry is not accessible for dyad **1** as there are no indications of an additional ultrafast process present in this molecule. The longer-lived lifetime obtained from a two exponential fit of the fluorescence upconversion data agrees well with the shortest lived component from the TCSPC measurements.

The main structural difference between **1** and **2** is the presence of the DMN component centrally placed in the linking bridge of **2**. An additional conformation of **2**, not available to **1**, which would lead to the ZnP−$C_{60}$ separation being reduced considerably, could arise from a structural distortion involving the DMN component of the bridge in which the DMN aromatic ring bends in an out-of-plane fashion, together with small distortions of the bridges, particularly at the cyclohexene group. As the ZnP and $C_{60}$ groups are attached onto the end of fairly long molecular arms, a small bend in the DMN ring would lead to considerable movement of the terminal chromophores relative to each other. A similar geometry has been observed in a giant U-shaped ZnP−DMN−NQ−methyl viologen ($MV^{2+}$) containing tetrad.[58] In this case, two ground state conformations are present: one where the bridge is in a relaxed state and the other where it has distorted (primarily through bending of the DMN and NQ groups) such that the terminal ZnP and $MV^{2+}$ chromophores are much closer.[63,66] A similar process has been identified as leading to considerably shortened CS lifetimes in some other trichromophoric donor−acceptor molecules where harpooning occurs to bring the charged ends closer.[67,68] Although there is

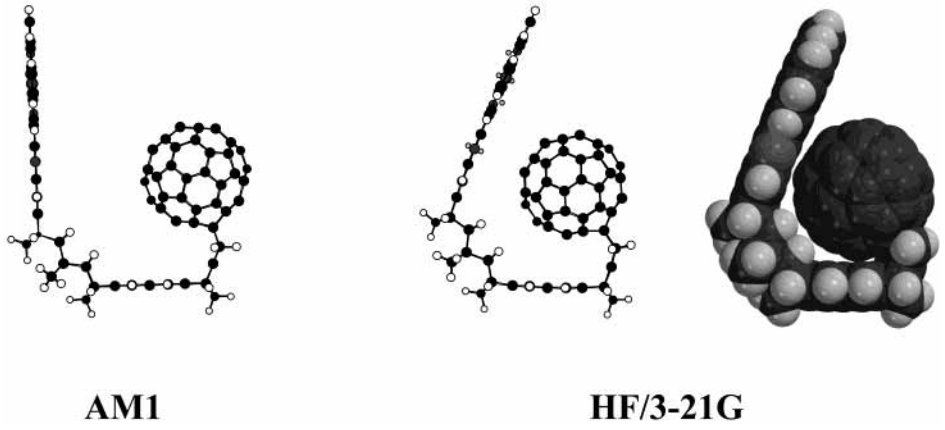


**Figure 8.** Profiles of the AM1 (left) and HF/3-21G (center and right) optimized structure of **2**. In this conformation, the ZnP and $C_{60}$ chromophores are only 4.0 Å apart at their closest separation. The space-filling representation of the HF/3-21G structure for **2** (right) reveals almost van der Waals contact between the $C_{60}$ and porphyrin groups.

no formal electrostatic force between the chromophore components of **2**, there may be an electronic attraction between the $C_{60}$ and ZnP groups which is not picked up by the AM1 calculations.[53] In fact, a number of recent experimental studies have confirmed that porphyrins and fullerenes are able to form intermolecular and intramolecular complexes, some with intercomponent separations less than the sum of the van der Waals radii of the individual components.[61,69−75] Ideally, this problem should be investigated by a quantum chemical method which includes electron correlation. However, the size of **2** puts such calculations beyond our computational resources. Nevertheless, the folded geometry of **2** in the gas phase was optimized using the ab initio HF/3-21G level.[76] Interestingly, the HF/3-21G folded geometry of **2** is substantially more compact than the corresponding AM1 relaxed geometry, predicting the smallest distance between the $C_{60}$ and porphyrin moieties to be only 4.0 Å, compared to 9.0 Å in the AM1 relaxed structure. This close distance is, indeed, achieved mainly by out-of-plane bending of the naphthalene ring system (see Figure 8). Only one folded conformation could be located at the HF/3-21G level. Presumably, an HF/3-21G extended conformation also exists, but this was not calculated because the HF/3-21G and AM1 geometries for this conformation are expected to be very similar to each other.

In summary, both HF/3-21G and AM1 theoretical models predict the existence of a single folded conformation in the gas phase. However, the two geometries are very different. The HF/3-21G relaxed geometry, hereafter referred to as the collapsed conformation, is much more compact than that predicted by the AM1 method. Indeed, the $C_{60}$ and zinc porphyrin groups are nearly in van der Waals contact of each other. This edge-to-edge interchromophore separation of 4.0 Å is certainly small enough to permit significant through space electronic coupling to occur between the two chromophores.[77,78]

The presence of a collapsed conformation is consistent with the experimental results and can explain the broadening observed in the ground-state absorption spectrum of **2** because of ground state interactions between the closely associated ZnP and $C_{60}$ chromophores. It was not possible, however, to resolve any identifiable CT absorption band. To exclude the alternate possibility that an intermolecular aggregate might be the source of the experimental observations, a solution of **2** in toluene was diluted through almost 2 orders of magnitude from 18 $\mu$M to 200 nM, and absorption spectra were recorded. All spectra were completely superimposable, indicating that intermolecular ground-state aggregation was not occurring.

Many of the experimental observations can be explained through the existence of a collapsed conformation of **2**. However, to account fully for all of the experimental results for this molecule, a model that comprises three distinct conformations of **2** is required. The three conformations are necessary to explain the existence of the two shortened lifetime components in the TCSPC fluorescence decay profiles of **2**, which arise from two EET processes, and the ultrafast subpicosecond decay component, which can be assigned to the PET process leading to CT emission. Although both AM1 and HF/3-21G theoretical models each appear to find only 1-folded conformer of **2**, the AM1 and HF/3-21G structures are significantly different, and it is possible that they represent distinct distorted and relaxed versions of the folded conformation of **2**. A more thorough ab initio MO search of the conformational space associated with the folded conformation of **2** will be undertaken in the hope of locating a second, less compact folded conformation akin to that predicted by the AM1 method. It is possible that solvent (toluene) plays an important role in stabilizing both folded conformations. So far, attempts to calculate solvation effects using continuum solvation models have been unsuccessful, because of failure of SCF convergence.

The experimental and computational evidence indicate that ultrafast PET between ZnP and $C_{60}$ is occurring in toluene in a collapsed conformation of **2** (i.e., an HF/3-21 folded geometry), whereas EET is the operative quenching mechanism in two other conformations of **2** (i.e., relaxed folded and extended conformations). Only the EET process is observed in both conformations of **1**. These conclusions can be reconciled by comparing the magnitude of the free energy change for charge separation, $\Delta G_{cs}$, for the various conformations. The free energy change may be estimated using the equation of Rehm and Weller:[79]

$$\Delta G_{cs} = e(E^{ox}(D) - E^{red}(A)) - E_{00} - X \qquad (1a)$$

where

$$X = \frac{e^2}{4\pi\epsilon_o\epsilon_s R_c} + \frac{e^2}{8\pi\epsilon_o}\left(\frac{1}{r^+} + \frac{1}{r^-}\right)\left(\frac{1}{\epsilon_{ref}} - \frac{1}{\epsilon_s}\right) \qquad (1b)$$

The $X$ term takes into account finite donor−acceptor separation, $R_c$, ionic radii, $r^+$ and $r^-$, and solvent dielectric constant, $\epsilon_s$. The oxidation potential of the ZnP donor, $E^{ox}(D)$, and the reduction potential of the $C_{60}$ acceptor, $E^{red}(A)$, were determined from electrochemical measurements in a 4:1 toluene/acetonitrile solution ($\epsilon_{ref} = 9.4$) to be +1.11 and −0.58 V, respectively.

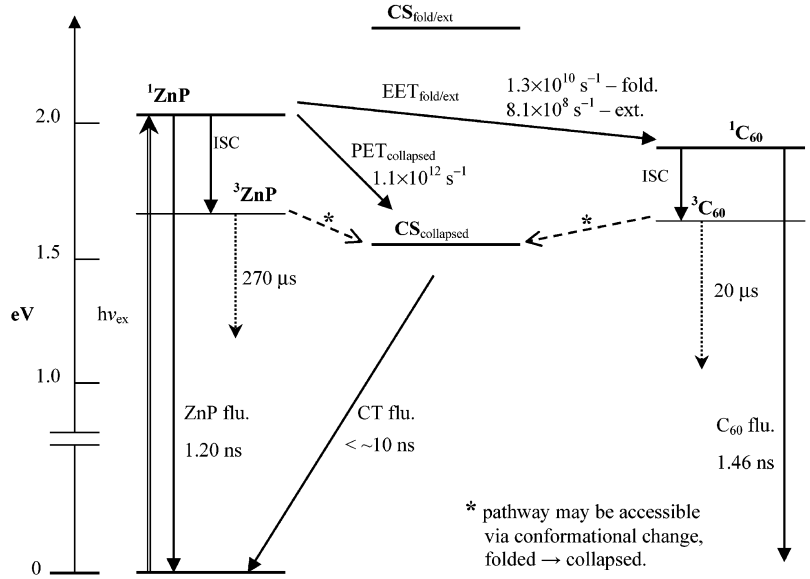


**Figure 9.** Energy level diagram summarizing the photophysical behavior of **2** in toluene.

$E_{oo}$, the lowest excited-state energy of ZnP, was obtained from the first absorption band of **3** (2.01 eV in benzonitrile and 2.03 eV in toluene). The AM1 (gas phase) center-to-center distances were used for $R_c$, and values for $r^+$ of 4.8 Å[80] and $r^-$ of 5.6 Å[26] were used.

Equation 1 predicts that PET is thermodynamically unfavorable ($\Delta G_{cs} > 0$) in toluene at the distances calculated for the separation of the ZnP and $C_{60}$ chromophores in the AM1-folded and extended conformations of **1** and **2**. Specifically, $\Delta G_{cs} =$ 0.30 eV at 20 Å, 0.2 eV at 15 Å, and 0.14 eV at 13.5 Å. However, the driving force for PET does become favorable ($\Delta G_{cs} < 0$) in toluene at chromophore separations of less than approximately 10 Å. At 8.5 Å (the center-to-center gas-phase separation for the HF/3-21G structure), the calculated driving force is −0.15 eV. Thus, at the close ZnP−$C_{60}$ separation of the collapsed conformation, direct through space PET becomes a favored deactivation pathway. Although the limitations in the application of eq 1b are known and absolute values for $\Delta G_{cs}$ are problematic, the trends indicated from these calculations for the effect of separation on the driving force for PET are consistent with the experimental observations. Of further interest are the shortened ZnP and $C_{60}$ triplet state lifetimes observed for **2** compared to **1** in toluene. This result suggests that, during the triplet state lifetime, the geometry of **2** is able to sample the collapsed conformation thus leading to an efficient charge-transfer process, to give the triplet CS state.[81]

In benzonitrile, the Rehm−Weller equation (eq 1) predicts an exergonic PET process for all conformations of **2**. The presence of a transient absorption that is characteristic of the $ZnP^{\bullet+}$ radical ion provides confirmation that PET is the dominant fluorescence quenching process. The rate constants for **2** in benzonitrile extracted from fluorescence lifetime data are $6.0 \times 10^9$ and $9.8 \times 10^8$ $s^{-1}$. Interestingly, the PET rate constant for the folded conformer is less than the EET rate constant found for this conformer in toluene ($1.3 \times 10^{10}$ $s^{-1}$). An increase in the end-to-end separation because of solvation of the chromophore in the polar solvent could make EET less competitive compared to superexchange mediated PET leading to this result. Although steady-state fluorescence quenching for **2** in benzonitrile indicates a quantum efficiency for the overall relaxation processes of 0.97, the rate constants extracted from TCSPC fluorescence lifetimes provide an estimated yield of 0.4. This discrepancy can again be attributed to the presence of the collapsed conformation providing an additional ultrafast (<20 ps) relaxation pathway. The reduced yield of the $ZnP^{\bullet+}$ transient at delayed times for **2** compared to **1** (cf. parts a and b of Figure 7) confirms that PET in the collapsed conformation must lead to ultrafast charge recombination. Thus, only the more extended conformations will lead to $ZnP^{\bullet+}$ with a lifetime detected by the nanosecond flash photolysis experiment. The major decay component of the transient absorption of **2** at 675 nm of 460 ± 50 ns is attributed to the $ZnP^{\bullet+}$ lifetime, whereas the minor long-lived contributions of 6 and 87 $\mu$s are assigned to the decay of some residual $^3$ZnP which also absorbs weakly at this wavelength. The two components can be assigned to the folded and extended conformations which have reduced lifetimes compared to the triplet lifetime of the ZnP model **3** (270 $\mu$s), because of different rates of conversion to the collapsed conformation and subsequent quenching by electron transfer.

## Conclusion

The excited-state processes occurring in **2** in toluene are summarized in the energy level diagram shown in Figure 9. The photophysical properties can be best explained if there are three conformations available to the molecule assigned as extended, folded, and collapsed. In toluene, the folded and extended conformers undergo EET with rate constants of $1.3 \times 10^{10}$ and $8.1 \times 10^8$ $s^{-1}$, respectively. In the collapsed conformer, PET occurs on a subpicosecond time scale to form a CS state characterized by CT fluorescence at 840 nm. In benzonitrile, PET is the dominant excited-state deactivation process for all conformations of **2**. For the extended conformations, PET leads to a CS state with a lifetime of 460 ns which is similar to that observed for **1**. However, the yield of the long-lived CS state of **2** is substantially reduced (~30%) compared to **1**. This decreased yield can be attributed to the presence of the additional collapsed conformer in **2** which provides a rapid relaxation pathway for a proportion of excited molecules. The novel and unusually complex photophysics exhibited in this work highlight the crucial role of molecular structure and conformation in influencing energy and electron-transfer processes in bridged donor−acceptor systems of this type.

**Acknowledgment.** This research was supported by Australian Research Council (ARC) grants to the K.P.G. and M.N.P.-

R. groups and an Australian Postgraduate Award to T.D.M.B. The award of an ARC Senior Research Fellowship to N.M.P.-R. is also acknowledged, as is the award of a Merit Allocation of computing time on the APAC National Facility. We thank Prof. Graham Fleming and Dr. Greg Scholes for their assistance and collaboration with the fluorescence upconversion measurement.

## References and Notes

(1) Closs, G. L.; Miller, J. R. *Science* **1988**, *240*, 440−447.
(2) Wasielewski, M. R. *Chem. Rev.* **1992**, *92*, 435.
(3) Gust, D.; Moore, T. A.; Moore, A. L. *Acc. Chem. Res.* **1993**, *26*, 198−205.
(4) Paddon-Row, M. N. *Acc. Chem. Res.* **1994**, *27*, 18−25.
(5) Bixon, M.; Jortner, J. *J. Chem. Phys.* **1997**, *107*, 5154−5170.
(6) Jortner, J.; Bixon, M. In *Electron Transfer−From Isolated Molecules to Biomolecules, Part 1*; Jortner, J., Bixon, M., Eds.; Wiley: New York, 1999.
(7) *Fullerenes*; Kadish, K. M., Ruoff, R. S., Eds.; Wiley: New York, 2000.
(8) Imahori, H.; Sakata, Y. *Adv. Mater.* **1997**, *9*, 537−546.
(9) Gust, D.; Moore, T. A.; Moore, A. L. *Res. Chem. Intermed.* **1997**, *23*, 621−651.
(10) Martin, N.; Sanchez, L.; Illescas, B.; Perez, I. *Chem. Rev.* **1998**, *98*, 2527−2547.
(11) Paddon-Row, M. N. *Fullerene Sci. Technol.* **1999**, *7*, 1151−1173.
(12) Imahori, H.; Sakata, Y. *Eur. J. Org. Chem.* **1999**, 2445−2457.
(13) Diederich, F.; Gomez-Lopez, M. *Chem. Soc. Rev.* **1999**, *28*, 263−277.
(14) Guldi, D. M. *Chem. Commun.* **2000**, 321−327.
(15) Guldi, D. M.; Prato, M. *Acc. Chem. Res.* **2000**, *33*, 695−703.
(16) Gust, D.; Moore, T. A.; Moore, A. L. *J. Photochem. Photobiol., B* **2000**, *58*, 63−71.
(17) Imahori, H.; Tamaki, K.; Yamada, H.; Yamada, K.; Sakata, Y.; Nishimura, Y.; Yamazaki, I.; Fujitsuka, M.; Ito, O. *Carbon* **2000**, *38*, 1599−1605.
(18) Guldi, D. M.; Maggini, M.; Martin, N.; Prato, M. *Carbon* **2000**, *38*, 1615−1623.
(19) Nierengarten, J. F.; Eckert, J. F.; Felder, D.; Nicoud, J. F.; Armaroli, N.; Marconi, G.; Vicinelli, V.; Boudon, C.; Gisselbrecht, J. P.; Gross, M.; Hadziioannou, G.; Krasnikov, V.; Ouali, L.; Echegoyen, L.; Liu, S. G. *Carbon* **2000**, *38*, 1587−1598.
(20) Schuster, D. I. *Carbon* **2000**, *38*, 1607−1614.
(21) Brabec, C. J.; Cravino, A.; Zerza, G.; Sariciftci, N. S.; Kiebooms, R.; Vanderzande, D.; Hummelen, J. C. *J. Phys. Chem. B* **2001**, *105*, 1528−1536.
(22) Shaheen, S. E.; Brabec, C. J.; Sariciftci, N. S.; Padinger, F.; Fromherz, T.; Hummelen, J. C. *Appl. Phys. Lett.* **2001**, *78*, 841−843.
(23) Foote, C. S. *Top. Curr. Chem.* **1994**, *169*, 347−363.
(24) Imahori, H.; Tkachenko, N. V.; Vehmanen, V.; Tamaki, K.; Lemmetyinen, H.; Sakata, Y.; Fukuzumi, S. *J. Phys. Chem. A* **2001**, *105*, 1750−1756.
(25) Imahori, H.; Hagiwara, K.; Akiyama, T.; Aoki, M.; Taniguchi, S.; Okada, T.; Shirakawa, M.; Sakata, Y. *Chem. Phys. Lett.* **1996**, *263*, 545−550.
(26) Bell, T. D. M.; Smith, T. A.; Ghiggino, K. P.; Ranasinghe, M. G.; Shephard, M. J.; Paddon-Row, M. *Chem. Phys. Lett.* **1997**, *268*, 223−228.
(27) Liddell, P. A.; Sumida, J. P.; Macpherson, A. N.; Noss, L.; Seely, G. R.; Clark, K. N.; Moore, A. L.; Moore, T. A.; Gust, D. *Photochem. Photobiol.* **1994**, *60*, 537−41.
(28) Lawson, J. M.; Oliver, A. M.; Rothenfluh, D. F.; An, Y.-Z.; Ellis, G. A.; Ranasinghe, M. G.; Kahn, S. I.; Franz, A. G.; Ganapathi, P. S.; Shephard, M. J.; Paddon-Row, M. N.; Rubin, Y. J. *J. Org. Chem.* **1996**, *61*, 5032−5054.
(29) Kuciauskas, D.; Lin, S.; Seely, G. R.; Moore, A. L.; Moore, T. A.; Gust, D.; Drovetskaya, T.; Reed, C. A.; Boyd, P. D. W. *J. Phys. Chem.* **1996**, *100*, 15926−15932.
(30) Imahori, H.; Hagiwara, K.; Aoki, M.; Akiyama, T.; Taniguchi, S.; Okada, T.; Shirakawa, M.; Sakata, Y. *J. Am. Chem. Soc.* **1996**, *118*, 11771−11782.
(31) Baran, P. S.; Monaco, R. R.; Khan, A. U.; Schuster, D. I.; Wilson, S. R. *J. Am. Chem. Soc.* **1997**, *119*, 8363−8364.
(32) Imahori, H.; Yamada, K.; Hasegawa, M.; Taniguchi, S.; Okada, T.; Sakata, Y. *Angew. Chem., Int. Ed. Engl.* **1997**, *36*, 2626−2629.
(33) Nierengarten, J.-F.; Schall, C.; Nicoud, J.-F. *Angew. Chem., Int. Ed.* **1998**, *37*, 1934−1936.
(34) Nierengarten, J.-F.; Nicoud, J.-F. *Chem. Commun.* **1998**, 1545−1546.
(35) Kuciauskas, D.; Liddell, P. A.; Lin, S.; Johnson, T. E.; Weghorn, S. J.; Lindsey, J. S.; Moore, A. L.; Moore, T. A.; Gust, D. *J. Am. Chem. Soc.* **1999**, *121*, 8604−8614.
(36) Schuster, D. I.; Cheng, P.; Wilson, S. R.; Prokhorenko, V.; Katterle, M.; Holzwarth, A. R.; Braslavsky, S. E.; Klihm, G.; Williams, R. M.; Luo, C. *J. Am. Chem. Soc.* **1999**, *121*, 11599−11600.
(37) Tamaki, K.; Imahori, H.; Sakata, Y.; Nishimura, Y.; Yamazaki, I. *Chem. Commun.* **1999**, 625−626.
(38) Guldi, D. M.; Luo, C.; Prato, M.; Dietel, E.; Hirsch, A. *Chem. Commun.* **2000**, 373−374.
(39) Williams, R. M.; Koeberg, M.; Lawson, J. M.; An, Y.-Z.; Rubin, Y.; Paddon-Row, M. N.; Verhoeven, J. W. *J. Org. Chem.* **1996**, *61*, 5055−5062.
(40) Liddell, P. A.; Kuciauskas, D.; Sumida, J. P.; Nash, B.; Nguyen, D.; Moore, A. L.; Moore, T. A.; Gust, D. *J. Am. Chem. Soc.* **1997**, *119*, 1400−1405.
(41) Kuciauskas, D.; Liddell, P. A.; Moore, A. L.; Moore, T. A.; Gust, D. *J. Am. Chem. Soc.* **1998**, *120*, 10880−10886.
(42) Carbonera, D.; Di Valentin, M.; Corvaja, C.; Agostini, G.; Giacometti, G.; Liddell, P. A.; Kuciauskas, D.; Moore, A. L.; Moore, T. A.; Gust, D. *J. Am. Chem. Soc.* **1998**, *120*, 4398−4405.
(43) Da Ros, T.; Prato, M.; Guldi, D.; Alessio, E.; Ruzzi, M.; Pasimeni, L. *Chem. Commun.* **1999**, 635−636.
(44) Fujitsuka, M.; Ito, O.; Imahori, H.; Yamada, K.; Yamada, H.; Sakata, Y. *Chem. Lett.* **1999**, 721−722.
(45) Martin, N.; Sanchez, L.; Guldi, D. M. *Chem. Commun.* **2000**, 113−114.
(46) Kuciauskas, D.; Liddell, P. A.; Lin, S.; Stone, S. G.; Moore, A. L.; Moore, T. A.; Gust, D. *J. Phys. Chem. B* **2000**, *104*, 4307−4321.
(47) Bahr, J. L.; Kuciauskas, D.; Liddell, P. A.; Moore, A. L.; Moore, T. A.; Gust, D. *Photochem. Photobiol.* **2000**, *72*, 598−611.
(48) Luo, C.; Guldi, D. M.; Imahori, H.; Tamaki, K.; Sakata, Y. *J. Am. Chem. Soc.* **2000**, *122*, 6535−6551.
(49) Imahori, H.; Tamaki, K.; Guldi, D. M.; Luo, C.; Fujitsuka, M.; Ito, O.; Sakata, Y.; Fukuzumi, S. *J. Am. Chem. Soc.* **2001**, *123*, 2607−2617.
(50) Fukuzumi, S.; Imahori, H.; Yamada, H.; El-Khouly, M. E.; Fujitsuka, M.; Ito, O.; Guldi, D. M. *J. Am. Chem. Soc.* **2001**, *123*, 2571−2575.
(51) Imahori, H.; Guldi, D. M.; Tamaki, K.; Yoshida, Y.; Luo, C.; Sakata, Y.; Fukuzumi, S. *J. Am. Chem. Soc.* **2001**, *123*, 6617−6628.
(52) The first bond of the $C_{60}$ cage is included in the bridge length.
(53) Jolliffe, K. A.; Langford, S. J.; Ranasinghe, M. G.; Shephard, M. J.; Paddon-Row, M. N. *J. Org. Chem.* **1999**, *64*, 1238−1246.
(54) The magnitude of the contribution of the superexchange interaction is currently under investigation and will be reported separately.
(55) Shephard, M. J.; Paddon-Row, M. N. *Aust. J. Chem.* **1996**, *49*, 395−403.
(56) Ranasinghe, M. G.; Oliver, A. M.; Rothenfluh, D. F.; Salek, A.; Paddon-Row, M. N. *Tetrahedron Lett.* **1996**, *37*, 4797−4800.
(57) Ghiggino, K. P.; Smith, T. A. *Prog. React. Kinet.* **1993**, *18*, 375.
(58) Jolliffe, K. A.; Bell, T. D. M.; Ghiggino, K. P.; Langford, S. J.; Paddon-Row, M. N. *Angew. Chem., Int. Ed. Engl.* **1998**, *37*, 916−919.
(59) Frisch, M. J.; Trucks, G. W.; Schlegel, H. B.; Scuseria, G. E.; Robb, M. A.; Cheeseman, J. R.; Zakrzewski, V. G.; Montgomery, J. A., Jr.; Stratmann, R. E.; Burant, J. C.; Dapprich, S.; Millam, J. M.; Daniels, A. D.; Kudin, K. N.; Strain, M. C.; Farkas, O.; Tomasi, J.; Barone, V.; Cossi, M.; Cammi, R.; Mennucci, B.; Pomelli, C.; Adamo, C.; Clifford, S.; Ochterski, J.; Petersson, G. A.; Ayala, P. Y.; Cui, Q.; Morokuma, K.; Malick, D. K.; Rabuck, A. D.; Raghavachari, K.; Foresman, J. B.; Cioslowski, J.; Ortiz, J. V.; Stefanov, B. B.; Liu, G.; Liashenko, A.; Piskorz, P.; Komaromi, I.; Gomperts, R.; Martin, R. L.; Fox, D. J.; Keith, T.; Al-Laham, M. A.; Peng, C. Y.; Nanayakkara, A.; Gonzalez, C.; Challacombe, M.; Gill, P. M. W.; Johnson, B. G.; Chen, W.; Wong, M. W.; Andres, J. L.; Head-Gordon, M.; Replogle, E. S.; Pople, J. A. *Gaussian 98*, revision A.7; Gaussian, Inc.: Pittsburgh, PA, 1998.
(60) Imahori, H.; El-Khouly, M. E.; Fujitsuka, M.; Ito, O.; Sakata, Y.; Fukuzumi, S. *J. Phys. Chem. A* **2001**, *105*, 325−332.
(61) Armaroli, N.; Marconi, G.; Echegoyen, L.; Bourgeois, J.-P.; Diederich, F. *Chem. Eur. J.* **2000**, *6*, 1629−1645.
(62) Tkachenko, N. V.; Guenther, C.; Imahori, H.; Tamaki, K.; Sakata, Y.; Fukuzumi, S.; Lemmetyinen, H. *Chem. Phys. Lett.* **2000**, *326*, 344−350.
(63) Bell, T. D. M.; Jolliffe, K. A.; Ghiggino, K. P.; Oliver, A. M.; Shephard, M. J.; Langford, S. J.; Paddon-Row, M. N. *J. Am. Chem. Soc.* **2000**, *122*, 10661−10666.
(64) The transient absorption spectrum of **1** was originally recorded in a point-by-point fashion and reported in ref 26. The spectra shown in Figure 7b have since been recorded using the YAG/OPO/ICCD apparatus installed at the University of Melbourne and are included for comparison and reference purposes.
(65) Experiment undertaken in collaboration with Prof. Graham Fleming and Dr. Greg Scholes at the University of California, Berkeley, USA. A

two exponential fit of a fluorescence upconversion decay profile gave 880 fs (42%) and 80 ps (58%) components.

(66) Shephard, M. J.; Paddon-Row, M. N. *J. Phys. Chem. A* **1999**, *103*, 3347−3350.

(67) Koeberg, M.; de Groot, M.; Verhoeven, J. W.; Lokan, N. R.; Shephard, M. J.; Paddon-Row, M. N. *J. Phys. Chem. A* **2001**, *105*, 3417−3424.

(68) Shephard, M. J.; Paddon-Row, M. N. *J. Phys. Chem. A* **2000**, *104*, 11628−11635.

(69) Konarev, D. V.; Neretin, I. S.; Slovokhotov, Y. L.; Yudanova, E. I.; Drichko, N. y. V.; Shul'ga, Y. M.; Tarasov, B. P.; Gumanov, L. L.; Batsanov, A. S.; Howard, J. A. K.; Lyubovskaya, R. N. *Chem.−Eur. J.* **2001**, *7*, 2605−2616.

(70) Sun, D.; Tham, F. S.; Reed, C. A.; Chaker, L.; Burgess, M.; Boyd, P. D. W. *J. Am. Chem. Soc.* **2000**, *122*, 10704−10705.

(71) Boyd, P. D. W.; Hodgson, M. C.; Rickard, C. E. F.; Oliver, A. G.; Chaker, L.; Brothers, P. J.; Bolskar, R. D.; Tham, F. S.; Reed, C. A. *J. Am. Chem. Soc.* **1999**, *121*, 10487−10495.

(72) Evans, D. R.; Fackler, N. L. P.; Xie, Z.; Rickard, C. E. F.; Boyd, P. D. W.; Reed, C. A. *J. Am. Chem. Soc.* **1999**, *121*, 8466−8474.

(73) Olmstead, M. M.; Costa, D. A.; Maitra, K.; Noll, B. C.; Phillips, S. L.; Van Calcar, P. M.; Balch, A. L. *J. Am. Chem. Soc.* **1999**, *121*, 7090−7097.

(74) Balch, A. L.; Olmstead, M. M. *Coord. Chem. Rev.* **1999**, *185*−*186*, 601−617.

(75) Tashiro, K.; Aida, T.; Zheng, J.-Y.; Kinbara, K.; Saigo, K.; Sakamoto, S.; Yamaguchi, K. *J. Am. Chem. Soc.* **1999**, *121*, 9477−9478.

(76) All geometry optimisations were carried out on a less substituted analogue of **2**, in which the four 3,5-di-*tert*-butylphenyl substituents of the zinc porphyrin and the two methoxy substituents of the naphthalene are replaced by hydrogen atoms.

(77) Balaji, V.; Ng, L.; Jordan, K. D.; Paddon-Row, M. N.; Patney, H. K. *J. Am. Chem. Soc.* **1987**, *109*, 6957.

(78) Paddon-Row, M. N.; Jordan, K. D. In *Modern Models of Bonding and Delocalization*; Liebman, J. F., Greenberg, A., Eds.; VCH Publishers: New York, 1988; Vol. 6, pp 115−194.

(79) Weller, A. *Z. Phys. Chem., Neue Folge* **1982**, *133*, 93.

(80) Degraziano, J. M.; Macpherson, A. N.; Liddell, P. A.; Noss, L.; Sumida, J. P.; Seely, G. R.; Lewis, J. E.; Moore, A. L.; Moore, T. A.; Gust, D. *New J. Chem.* **1996**, *20*, 839−851.

(81) The energies of the ZnP and $C_{60}$ triplet states were determined from phosphorescence measurements of the model compounds **3** and **4** in a methylcyclohexane glass at 77 K. The values found were 1.60 eV for $^3$ZnP and 1.58 eV for $^3C_{60}$. The onset of the CT fluorescence band at 810 nm of **2** in toluene corresponds to an energy of 1.54 eV. Thus, PET from $^3$ZnP and $^3C_{60}$ is thermodynamically feasible. In the folded and extended arrangements, the ZnP−$C_{60}$ separation is most likely too great for significant PET from these triplet states, but conversion to the collapsed conformation is the source of the quenched triplet state lifetimes of **2** in both toluene and benzonitrile.